| | |
|---|---|
| ***Number*** | 173 |
| ***Publication Year*** | 2022 |
| ***Acceptance in OA@INAF*** | 2022-07-11T10:33:19Z |
| ***Title*** | BC-SIM-TN-009_STC_GM_Observation_Strategy_Optimization_2022 |
| ***Authors*** | SIMIONI, EMANUELE; RE, Cristina; Da Deppo, Vania; ZUSI, MICHELE; CAPACCIONI, FABRIZIO; CAPRIA, MARIA TERESA; Alain Doressundiram; Yves Langeven; PALUMBO, PASQUALE; Mathieu Vincendon; CREMONESE, Gabriele |
| ***Affiliation of first author*** | O.A. Padova |
| ***Handle*** | http://hdl.handle.net/20.500.12386/32466; https://doi.org/10.20371/INAF/TechRep/173 |

# BC-SIM-TR-009 STC GM Optimization Report Issue 1.0

Emanuele Simioni[1], Cristina Re[1], Vania Da Deppo[2], Michele Zusi[3]
Fabrizio Capaccioni[3], Maria Teresa Capria[3], Alain Doressundiram[4], Yves Langeven[5], Pasquale Palumbo[6], Mathieu Vincendon[5], Gabriele Cremonese[1]

[1]INAF-OAPd, Vicolo Osservatorio 5,35122, Padua, Italy
[2]INAF-CNR via Trasea 7, 35131, Padua, Italy
[3]INAF-IAPS, Via Fosso del Cavaliere 100, 00133, Rome, Italy
[4]OLESIA (Observatoire de Paris, Laboratoire d'Études Spatiales et d'Instrumentation en Astrophysique), 92195 Meudon Cedex, France
[5]CNRS (Institut d'Astrophysique Spatiale), Université Paris Sud, 91405, Orsay, France
[6]Università Parthenopea, Centro Direzionale Isola 4, 80133, Naples, Italy

# Index

## Approvation

| | |
|---|---|
| **Edited by:** | Emanuele Simioni |
| | |
| **Approved by:** | Gabriele Cremonese |
| | |

## Change Log

| Issue | Revision | Date | Affected Pages | Change description |
|---|---|---|---|---|
| **0** | 0 | 23/09/2021 | All | Draft |
| **1** | 0 | 06/07/2022 | All | First Versions |
| | | | | |
| | | | | |

# 1 Introduction

## 1.1 Scope

The present document has been issued to describe the optimization of the Global Mapping Observation strategy of STC, channel of the Spectrometers and Imagers for MPO BepiColombo Integrated Observatory SYStem (SIMBIO-SYS). These optimization has the scope to ensure the performance and the objectives of the STC Channel reducing the DV in manner to make available more targets acquisitions for HRIC or a greater flexibility for VIHI channel.

## 1.2 Reference Document

[RD. 1] BC-SIM-TN-003_-_Reports_and_Note_Layout_and_Flow, 10.20371/INAF/TechRep/36

[RD. 2] BC-SIM-TN-002-STC_Observation_Strategy_Issue1_Rev4, 10.20371/INAF/TechRep/35

[RD. 3] BC-SIM-GAF-MA-002 rev.8_SIMBIO-SYS FM User Manual, 2017

[RD. 4]EGSE

[RD. 5] BC-SIM-TN-001 FOPs_Decription_Issue1 (http://dx.doi.org/10.20371/INAF/TechRep/15)

[RD. 6]NECP

[RD. 7]BC-SIM-TN-004_-_SIMBIO-SYS_FOP_update_after_NECP, 10.20371/INAF/TechRep/58

[RD. 8] BC-SGS-PO-002_v3_0_A_BepiColombo_Science_Overview_2020Jun10

## 1.3 Acronyms

| | |
|---|---|
| **ACK** | Acknowledgment |
| **ADC** | Analogical Digit Converter |
| **APID** | Application Process IDentifier |
| **ASW** | Application SoftWare |
| **CM** | Color Mode |
| **CSV** | Comma Separated Values |
| **DSNU** | Dark Signal not Uniformity |
| **DV** | Data Volume |
| **FOP** | Flight Operation Procedure |
| **FPA** | Focal Plane Assembly |
| **HK** | Housekeeping |
| **HRIC** | High spatial Resolution Imaging Channel |
| **ICO** | Instrument Checkout |
| **IT** | Integration Time |
| **ME** | Main Electronics |

| | |
|---|---|
| **NECP** | Near Earth Commissioning Phase |
| **OBCP** | On-Board Control Procedure |
| **OB** | Optical Bench |
| **OBSW** | On Board Software |
| **PDOR** | Payload Direct Operation Request |
| **PDS** | Planetary Data System |
| **PE** | Proximity Electronics |
| **PNG** | Portable Network Graphics |
| **PSC** | Packet Sequence Control |
| **PSS** | Simbiosys TC Parameter |
| **RT** | Repetition Time |
| **SIMBIO-SYS** | Spectrometers and Imagers for MPO BepiColombo Integrated Observatory SYStem |
| **SSC** | Source Sequence Count |
| **SSMM** | Solid State Mass Memory |
| **STC** | STereo imaging Channel |
| **S/C** | Space-Craft |
| **SK** | Spice Kernels |
| **TAA** | True Anomaly Angle |
| **TC** | TeleCommand |
| **TEC** | Thermo-Electric Cooler |
| **TM** | Telemetry |
| **VIHI** | VIsible and Hyper-spectral Imaging channel |
| **XML** | eXtensible Markup Language |

## 1.4 Document Format and Repository

This document is compliant with the SIMBIO-SYS Report and Note Layout and Flow [RD. 1] and will be archived both on the INAF Open Access repository and the SIMBIO-SYS team Archive.

## 1.5 Document Organization

This document is organized in sections whose topics are listed as follows:

- Section 2 will describe the Optimization Pipeline adopted;
- Section 3 will export the constraints imposed by the payload;
- Section 4 will delineate the list of parameters optimized: orbit segmentation, AT overlapping, CT overlapping. For each parameter a section will describe the assumptions adopted and a section will show the result of the analysis;
- Section 5 will describe the result of the DV calculation while Section 6 will summarize as appendix the Data Rate assumption adopted.

# 2 Optimization pipeline

STC Observation strategy [RD. 2] has reported the first design of the Observation strategy both for the Color Mode and Global Mapping for STC Stereo Channel.
Different issues were optimized in the last years to reduce the DV (Data Volume) simplifying the strategy and allowing the same performances.
Due to the flexibility of its design, in order to properly operate STC, some parameters must be defined: filters combination, window size in pixels to be acquired for each filter, repetition time and compression factor. In order to save the DV and simplify the instrument operations and its implementation in the telecommands it is convenient to divide a spacecraft orbit around Mercury in segments.
**Note: The number of the segments could be increased in order to optimize the use of the IT and the DV.**
Report [RD. 2] assumes that the MPO orbit is divided in 11 segments: in 9 of them STC will work acquiring both the sub-channels. In the last 2 segments (near the poles when the nadir of SIMBIO-SYS is pointing to latitudes greater or less than ±83°), only one sub-channel will work, i.e. the one looking at the illuminated Mercury surface.
This report has as first goal to describe the impact of the number of orbit segments on the optimization of the instrument performances and DV.

The optimization process will proceed as follows:

- Definition of a SK (Spice Kernels) based dataset;
- Evaluation on the basis of the design parameters of the PSS (**Simbiosys TC Parameter**) and timeline;
- Simulation to estimate DV.

The optimization process follows the diagram of **Figure 1** applied to all the Aphelion (or its subset) orbits, the document organization respects this process overflow.

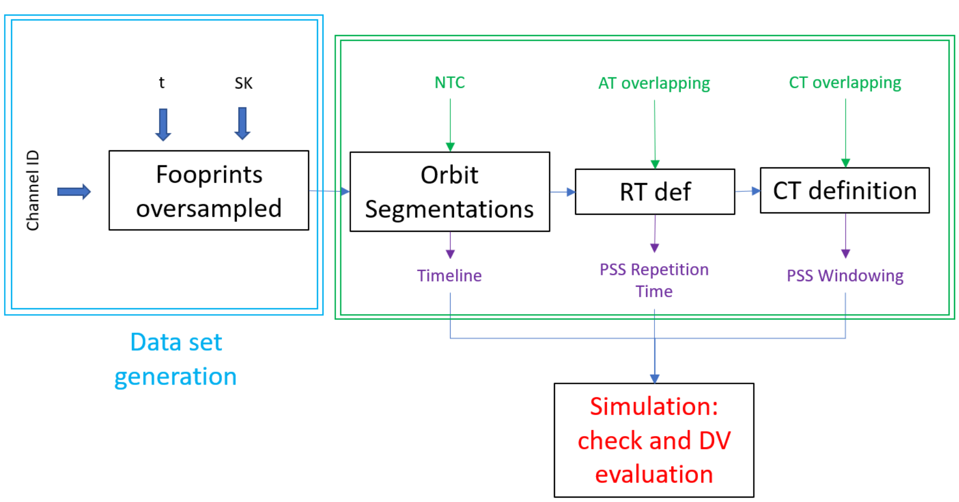


**Figure 1** *Optimization process pipeline*

The tool developed is based on MATLAB and exploits the SK.
The starting point (blue square) is the generation of a dataset for a particular phase of the mission. This dataset is the result of an oversampling of the SK data to a minimal time step (in case of STC:1 second) of:

- the footprints of the channels of the instrument
- the illumination conditions
- the boresight on ground intercept and its velocity

The dataset generation allows to provide all the information derived by Spice Kernels needed for strategy optimization.
Second phase (green) is the effective optimization of the timeline (orbit segmentation and strategy) and of the PSS (commanded paramters) to guarantee the input required (defined here as Number of TC, AT overlapping and CT overlapping).
Once all these parameters are defined for each segment of every orbit of the phase considered (for example one Aphelion), the same TCs are simulated to follow the requirements and the evaluation of the DV and the Data Rate as described in Appendix (Section 6).

# 3 CONSTRAINTS FROM THE INSTRUMENT DESIGN

## 3.1 Field of view and Channels

STC is composed of two sub-channels (i.e. High (-H) and Low (-L)). The angle between each sub-channel line of sight and the instrument boresight is nominally 20° (see **Figure 2**).

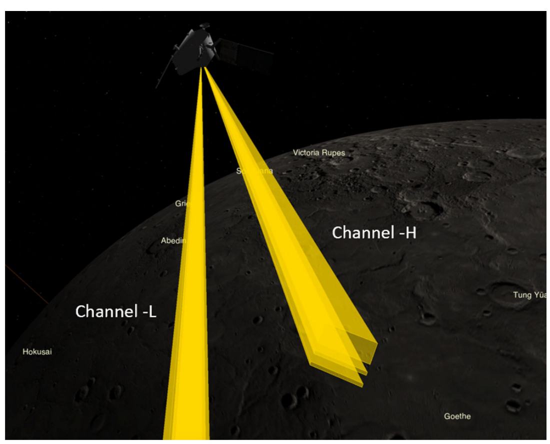


**Figure 2** *Screenshot of Cosmographia Tools showing the two sub-channels FoVs of STC. For the sub-channel-H, it is possible to note the FoVs of the Panchromatic filter (greater one) and the 2 colour filters.*

The two sub-channels images are acquired on the same detector (2048 x 2048 pixels). The field of view (FoV) of each sub-channel is rectangular, being 5.386° in the cross-track (CT) direction and 4.8° in the along-track (AT) direction including gaps (Figure 4 and Table 1).

Three filter strips for each sub-channel, one panchromatic and 2 broad bands, form a window (Filter Strip Assembly) mounted in front of the detector:

- The 4 broad band filters are centered at the wavelengths of 420 nm, 550 nm, 750 nm and 920 nm and have a bandwidth of 20 nm; the maximum FoV is 5.39° x 0.38° (896 x 64 pixels).
- The panchromatic filters (see **Figure 3** ) are centered at the wavelength of 700 nm and have a bandwidth of 200 nm; the FoV is on average 5.38° x 2.31° (896 x 384 pixels); the angle between each panchromatic filter line of sight and the instrument boresight is 21.375°.

**For both the Panchromatic and broad band filters the radiometric calibration is guaranteed only for the central part, i.e. 768 pixels in CT direction (corresponding to 4.61°).**

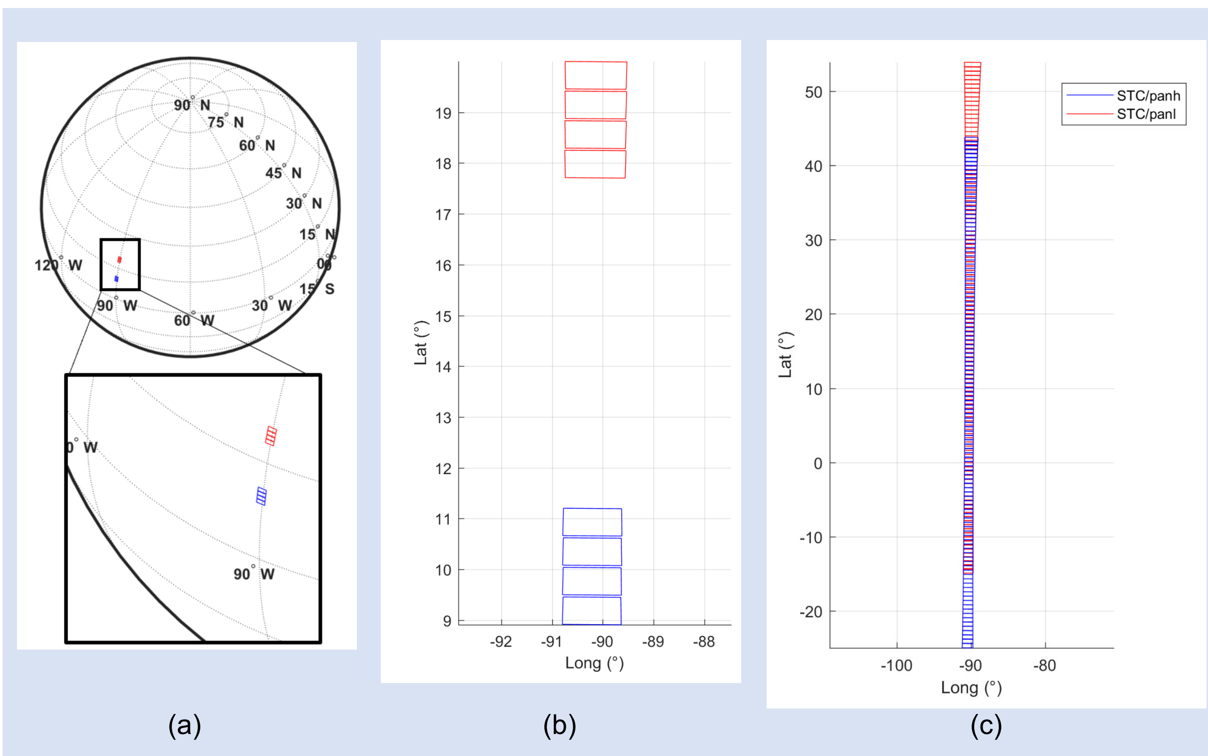


**Figure 3** – Projection on the surface of Mercury, at the periherm of Aphelion 0, of the footprints (FoVs) of the panchromatic filter of SIMBIO-SYS: STC –PAN H and -L (respectively in blue and red). Simulations: in a) projection on the Mercury sphere and in b) equirectangular projection, of 4 consecutive acquisitions with a repetition time of 10 sec (which does not guarantee the AT overlapping). In (c) same simulation but extended to 10 minutes around the periherm visualized with the same axis scale factor.

## 3.2 STC Detector

Due to its orbit in close proximity to the Sun, the BepiColombo spacecraft with its payload will work in a harsh environment due to radiation dose and heat production. Thus, thanks to its intrinsic radiation hardness and good performances at high temperatures, a CMOS detector has been chosen for STC. .

The detector has been developed by Raytheon Vision Systems (RVS) that has produced a custom visible sensor based on a 2048 × 2048 format with a 10 μm pitch unit cell. The same device has been selected also for the SIMBIO-SYS HRIC and for the Colour and Stereo Surface Imaging System (CaSSIS) for the ExoMars Trace Gas Orbiter mission.

Detector ROIC implementation and CU interface limit the possible combination of windowing dimensions: both AT and CT **can be commanded only as multiple of 64 px with a minimum possible window acquisition of 64x128 pixels (HxW).**

The instantaneous field of view (IFoV) of each pixel depends on its position with respect to the boresight of the channel; it is on average 105 x 105 μrad.

On the detector a Window X (64x128 pixels outside the illuminated area) is acquired for calibration purposes, nominally with the same compression factor used to acquire the other filters .

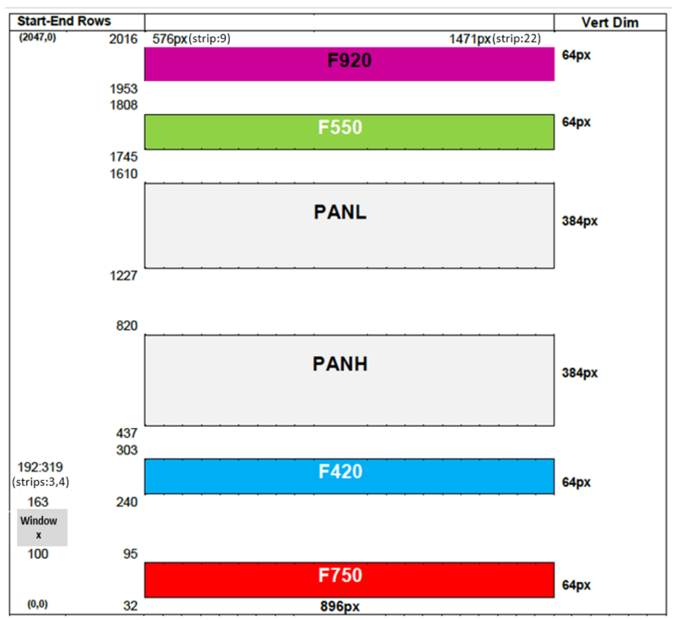


**Figure 4 -** Position of the filter regions on the detector. Vertical coordinates are expressed in pixels. Horizontal coordinates are expressed in pixels and in "strips" (1 strip=64 pixels)

A summary of the filter coordinates on the detector and the associated FoV is reported in the following table.

| | Raw Definition | | Dimension | Bsight Dir | FoV | Angle Definition (vs Nadir) | | Angle Definition (vs +-20°) | | Bsight (vs ±20°) |
|---|---|---|---|---|---|---|---|---|---|---|
| | Starting | End | | | | Starting | End | Starting | End | |
| | [px] | [px] | [px] | [°] | [°] | [°] | | | | [°] |
| F750 | 32 | 95 | 64 | 17.95 | 0.38 | 17.76 | 18.14 | -2.24 | -1.86 | -2.05 |
| GAP | 96 | 239 | 144 | 18.585 | 0.87 | 18.15 | 19.02 | -1.85 | -0.98 | -1.42 |
| F420 | 240 | 303 | 64 | 19.22 | 0.38 | 19.03 | 19.41 | -0.97 | -0.59 | -0.78 |
| GAP | 304 | 436 | 133 | 20.2975 | 0.81 | 19.89 | 20.70 | -0.11 | 0.70 | 0.30 |
| PANH | 437 | 820 | 384 | 21.375 | 2.31 | 20.22 | 22.53 | 0.22 | 2.53 | 1.38 |
| GAP | 821 | 1226 | 406 | - | - | - | - | - | - | |
| PANL | 1227 | 1610 | 384 | 21.375 | 2.31 | 20.22 | 22.53 | 0.22 | 2.53 | 1.38 |
| GAP | 1611 | 1744 | 134 | 20.2975 | 0.81 | 19.89 | 20.70 | -0.11 | 0.70 | 0.30 |
| F550 | 1745 | 1808 | 64 | 19.22 | 0.38 | 19.03 | 19.41 | -0.97 | -0.59 | -0.78 |
| GAP | 1809 | 1952 | 144 | 18.585 | 0.87 | 18.15 | 19.02 | -1.85 | -0.98 | -1.42 |
| F920 | 1953 | 2016 | 64 | 17.95 | 0.38 | 17.76 | 18.14 | -2.24 | -1.86 | -2.05 |

**Table 1**- Definition of the starting and ending vertical coordinates of the filter region on the detector in terms of pixels and FoV. The FoV is defined for each pixel row both in the nadiral reference system (angles on ground) and in the local sub-channel reference system where -H and -L are considered with a nadiral angle of 20°. All filters are considered horizontally starting from pixel 576 to 1472 with a FoV of 5.38° centered in the nadir direction.

# 4 STC Typical orbit

STC operates in GM only at Aphelion (TAA=138°-222°) The planet in this phase covers a mean of 0.28°of TAA for each S/C orbit. Illumination conditions at Aphelion obliges the instrument to work in this phase around the periherm. **Figure 5** shows a typical GM orbit divided in operation segments; we assume an available number of TCs equal to N.

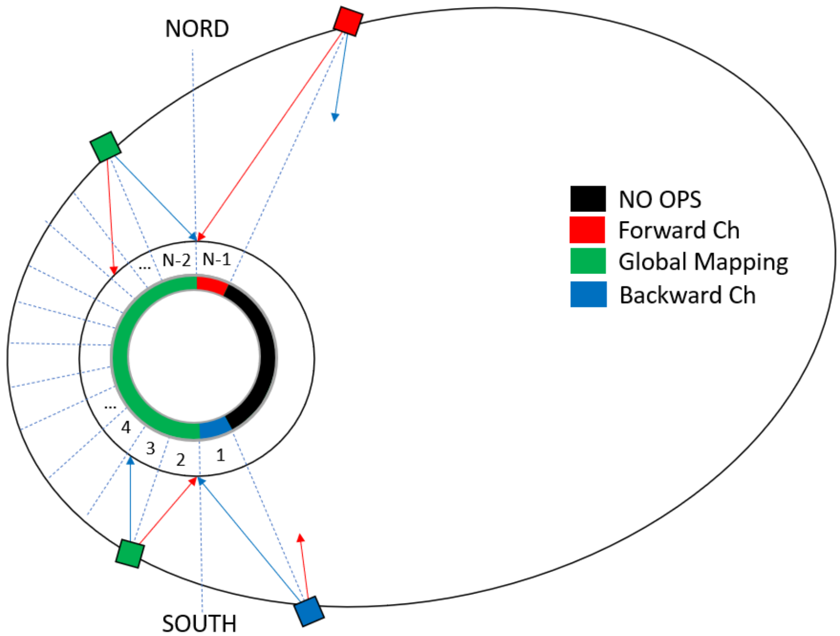


**Figure 5** *Subdivision in segments for an MPO aphelion orbit. For e ach segment STC is represented in red, blue, green depending on whether it is working, respectively, with the single forward or backward channel, or both channels.*

Considering that each time the MPO will flip around its axis (2 times every mercury year) the channel oriented in the same direction of the S/C velocity will change; thus we do not refer to channels as PAN-H or PAN-L but forward or backward.
This has an obvious impact in the CT overlapping calculation where it must be considered that in the orbit at aphelion, closest to sun, the overlapping must be considered for the channel HIGH with the channel LOW and viceversa.
GM orbit starts with the forward (PAN-H or PAN-L depending on the True Anomaly) channel acquisition between the moment of the intercept of the terminator (near the pole) by the PAN boresight until the other channel boresight reaches the south pole.
The Following orbit segment works in GM with both the channels. The last segment covers the time when the forward channel arrives on the line separating the illuminated and the dark hemisphere and when the backward channel achieves the same line. This last segment ends with the last stop TC.
Orbit segments division is described in detail in the next section.

| TC-N | Mode | Fop ID | Fop Names |
|---|---|---|---|
| 1 | Backward Ch | ASSF301/ ASSF302 | STC Science SURF SINGLE PANH /L |
| 2 / (N-2) | GM | ASSF307 | STC Science SURF NOMINAL GM |
| (N-1) | Forward C | ASSF302/ ASSF301 | STC Science SURF SINGLE PANL/H |
| N | Stop | SS-FCP-368 | STC STOP SCIENCE |

**Table 2** TCs commanded during a typical orbit of STC and the FOPs to be commanded.

**Table 2** reports the functional operation procedures (see [RD. 7] for definitions) associated with the different orbit segments.

In the case of Aphelion, note that the MPO flip, maneuver applied at each Aphelion, obliges the use, during single channel acquisition, only PANL (in the case of first Aphelion) (which represent the forward channel in this phase) before the TA 180 and PANH after TA 180.

## 4.1 Segment Orbit definition

### 4.1.1 Assumptions

Considering the purpose of the instrument to perform a complete GM in stereo mode we assume, as best solution, the orbit segments as function of the subnadiral latitudes defined constant for each aphelion. Although the drift of the periherm and the change in height will allow to have a uniform data set to be used to apply photogrammetry.
The subnadiral latitude range for an orbit could be encountered in two events: both when the boresight overpasses the terminator for the first and for last science TC of each orbit. Considering all the GM phase we fix:

- the first subnadiral latitude as the max (evaluated for each orbit of the Aphelion) of the case at south pole in which both the channels are operative
- the last subnadiral latitude as the min of the cases at north pole.

Considering the Aphelion 1 phase (between 16-Jun-2026 00:00 and 16-Jul-2026 23:59), **Figure 6** shows the subnadiral latitude associated with the two events (associated to the first and last GM TCs of **Table 2**). Both the parameters have a variation less than 0.31° during the Aphelion.

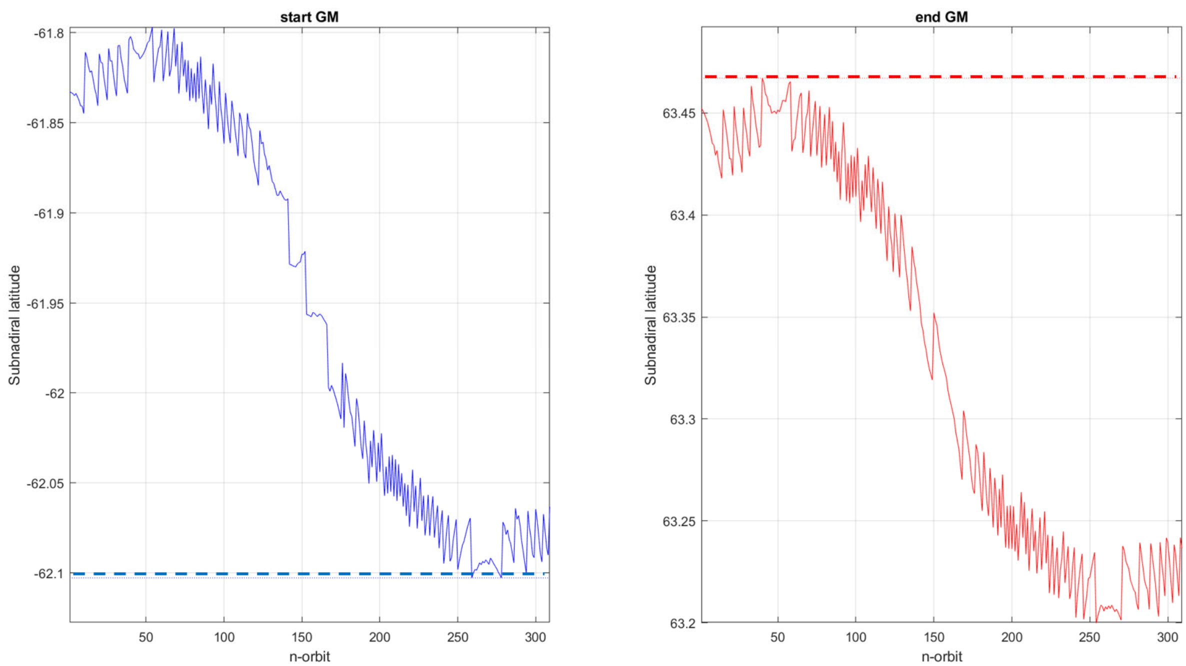


**Figure 6** *Definition of the beginning and end of GM following SK (based on mk spice kernel: bc_plan_v271_20210802_001.tm) for each orbit of Aphelion 1 phase. Dot line represents the minimum value for the GM starting and max value for GM stop (for this Aphelion 62.1027S and 63.4669N).*

○

### 4.1.2 Analysis

The TC reported in **Table 2** can be fixed by the following definitions and equations.

| TC-N | Mode |
|---|---|
| | |
| 1 | Subnadiral latitude corresponding to the first occasion in the orbit in which the Forward Ch boresight intersects a region with incidence angle less than 90°. |
| 2 | Minimum subnadiral latitude (for all the Aphelion) corresponding to the first occasion in the orbit in which Backward Ch boresight intersects a region with incidence angle less than 90°. |
| i | Uniform division of the subnadiral latitudes $L_s(ntc)$ between $L_s(2)$ and $L_s(N-1)$ following equation: $$L_s(2) + (i-2)\,\frac{L_s(N-1) - L_s(2)}{N-3}$$ |
| (N-1) | Maximum subnadiral latitude (for all the Aphelion) corresponding to the first occasion in the orbit in which Forward Ch boresight intersects a region with incidence angle less than 90°. |
| N | Subnadiral latitude corresponding to the first occasion in the orbit in which the Backwa rd Ch boresight intersects a region with incidence angle greater than 90°. |

An example of the results of this definition for the first and last orbits of Aphelion 1 is reported in **Table 3.**

| | N-TC | Time | SubnadLat | Boresight Ch L | Boresight Ch H | TC |
|---|---|---|---|---|---|---|
| First orbit 2026 JUN 16 09:57:53 | 1 | 00:00:00 | -79.7307 | -89.9534 | NaN | STC-L |
| | 2 | 00:14:23 | -62.1027 | -55.2692 | -88.9031 | GM |
| | 3 | 00:20:13 | -44.1642 | -38.5481 | -49.747 | GM |
| | 4 | 00:25:39 | -26.2257 | -21.5255 | -30.9799 | GM |
| | 5 | 00:30:49 | -8.28715 | -4.0488 | -12.4783 | GM |
| | 6 | 00:35:52 | 9.65137 | 13.7027 | 5.55469 | GM |
| | 7 | 00:40:55 | 27.5899 | 31.8837 | 23.2761 | GM |
| | 8 | 00:46:09 | 45.5284 | 50.4172 | 40.6125 | GM |
| | 9 | 00:51:39 | 63.4669 | 69.3296 | 57.6055 | GM |
| | 10 | 00:58:04 | 82.7385 | 75.475 | 89.9354 | STC-H |
| | 11 | 01:03:53 | 81.3501 | NaN | 89.9478 | STOP |
| Last orbit 2026 JUL 16 17:28:41 | 1 | 00:00:00 | -79.9632 | NaN | -89.9467 | STC-H |
| | 2 | 00:14:04 | -62.1027 | -68.6742 | -55.5427 | GM |
| | 3 | 00:19:48 | -44.1642 | -49.5181 | -38.7784 | GM |
| | 4 | 00:25:09 | -26.2257 | -30.7442 | -21.684 | GM |
| | 5 | 00:30:16 | -8.28715 | -12.3567 | -4.2349 | GM |
| | 6 | 00:35:16 | 9.65137 | 5.67209 | 13.605 | GM |
| | 7 | 00:40:18 | 27.5899 | 23.3187 | 31.8143 | GM |
| | 8 | 00:45:31 | 45.5284 | 40.622 | 50.43 | GM |
| | 9 | 00:51:02 | 63.4669 | 57.5542 | 69.4042 | GM |
| | 10 | 00:57:27 | 82.6237 | 89.9312 | 75.2391 | STC-L |
| | 11 | 01:03:27 | 81.1367 | 89.9455 | NaN | STOP |

**Table 3** *Example of the orbits segments in the case of 11 TCs for orbit. The table reports for each TC the time with respect to the beginning of the orbit, the subnadiral point at the moment of the execution, the latitude of the intercept of the boresight of the two channels (when in an illuminated region ) and the kind of TC used corresponding to the FOP define in* **Table 2**.

Following the definition in **Table 3**, the subnadiral latitudes of the GM (here depicted in blue) are invariant with respect to the orbit of the Aphelion phase.

## 4.2 AT overlapping and Repetition Time

### 4.2.1 Assumptions

In the previous observation strategy (see [RD. 2]), the percentage of overlapping along-track (AT) between consecutive acquisitions of each channel was defined to be greater than 10%. Considering the experience gained with other push-frame instruments, in particular the Stereo Camera CASSIS, which is using the same detector of STC, we assume hereafter to fix as along track overlapping limit a number of pixel greater than 30 (the 7.8% of AT STC FoV).
These optimizations will reduce the DV in manner to make available more targets acquisitions for HRIC or a greater flexibility for VIHI channel.
This limit must be respected simultaneously by both the STC channels.
This overlapping will be useful for the alignment of the images obtained in following acquisitions, allowing the identification of a number of tie points in the overlapping area able to accomplish a stable image mosaicking. The availability of a continuous mosaicking of the PAN acquisitions would be important in order to guarantee a stable image block both for the 2D and 3D mapping.
For 3D-reconstruction purposes, the main process consists in the identification of the corresponding image points and in accurately measuring the image coordinates of these points in the overlapping areas within the stereo pair.
On the other side, the processing of a stereo pair might provide DTMs affected by vertical and lateral offsets between each other. This problem may be due to these offsets or tilts that are not well constrained by the limited surface coverage of the images. In fact, an absolute positioning of the DTMs is typically well constrained if large regional blocks of images are available.

### 4.2.2 Analysis

The RT can be evaluated as function of two parameters:

- The pixel on ground $pog(ch,t)$ which defines the along track dimension at a time $t$ of the pixel on ground defined by the channel $ch$
- The velocity $v_b(ch,t)$ of the intercept of the boresight defined as

$$v_b(ch,t) = \frac{\delta b}{\delta t}$$

Defined as the minimum repetition time operable in order to reach the minimum overlapping along track required for all the orbit segments considered and for both channels, the Repetition time can be defined as the minimum of the ratio of these two parameters with respect to the channel and the time of each orbit segment.

$$RT = OVER_{px}\, min_{ch,t}\left(\frac{pog(ch,t)}{v_b(ch,t)}\right)$$

Where $OVER_{px}$ is the minimum overlapping along track in pixel for both channels.

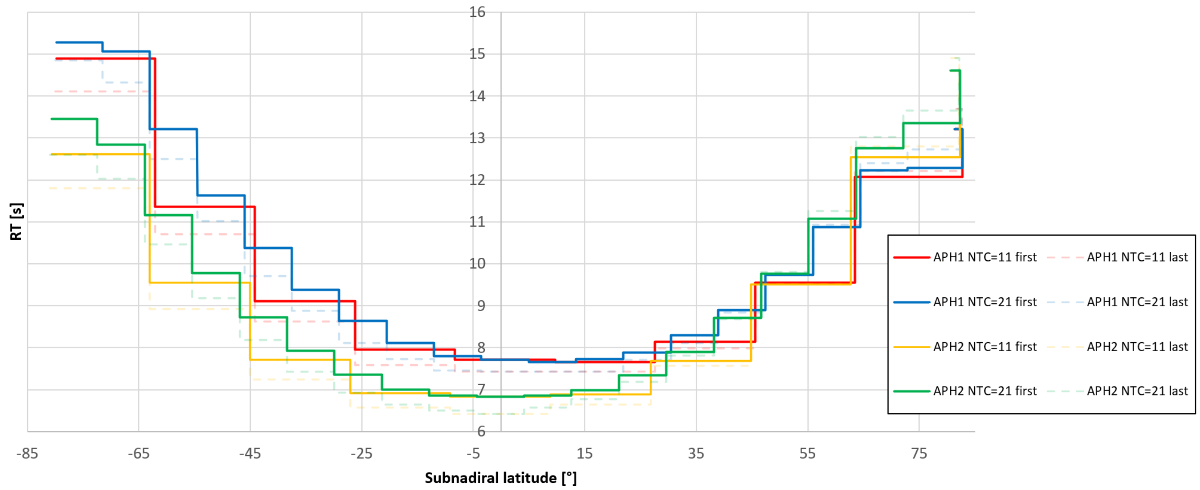


**Figure 7** Evaluation of the RT associated to the STC TCs as a function of the RT for the first (continue) and last (segmented) orbit of the Aphelion 1 and Aphelion 2 (12-Sep-2026 12-Oct-2026). In warmer colors (red and yellow) the evaluation for11 TCs and in colder colors (green and ble) 21 TCs.

**Figure 7** underlies the decrease of the RT during the Aphelion 1 between the first and the last orbit.
For the lower latitude using 21 TCs increases the RT of the 16% with the relative impact on the DV.
Considering that the $RT$ is defined as the minimum time to guarantee the overlapping for both the channels for a defined orbit segment, the number of TCs and the orbit segmentation have a strong impact on this parameter.

## 4.3 CT overlapping and CT dimension

### 4.3.1 Assumptions

Considering the across track configuration, in order to guarantee a sufficient number of interesting points in the overlapping areas of images to be mosaicked, even in this case we assume the same limit of 30 px between two consecutive orbits for each latitude.
This overlapping should be guaranteed for each latitude of the same acquisition.
In any case, an acquisition with the complete FoV could increase the accuracy in the global mosaicking. Considering that in GM the RT is always greater than 6 seconds and that the minimum RT introduced by the CU is always less than 0.4 seconds (see [RD. 2] for details) a predefined FOP could be defined to substitute the ASSF307 (see **Table 2**) with two call to the same FCP separated by 1 seconds, the first with maximal CT dimensions and the second with the required one.

As described in Section 3.2 algorithmic and physical constraints impose that the number of pixels both along and cross track be a multiple of 64 and that the minimum window CT size allowed be 128 pixels.
Considering a symmetrical acquisition CT this brings to an overconsumption which can be considered as a noise with a mean of 64 pixel for each acquisition and a standard deviation equal to $128/\sqrt{12}$.

### 4.3.2 Analysis

CT dimension is evaluated as the maximum between the two channels on the orbit sector (OS), following the equation:

$$CTdim^* = ((\frac{\alpha_{r\_orbit}}{(896 - overCT)} \frac{896}{\Delta Long}))$$

Where

- $\alpha_{r\_orbit}$ is the rotation of the planet (during a MPO orbit)
- $\Delta Long$ is the Cross Track coverage defined by Spice Kernels.
- $over$CT is the overlapping cross track in pixels (nominally 30 for the Global Mapping)

Note that CTdim must be rounded up considering that it must be a multiple of 128 assuming symmetrical acquisitions.

It is clear that for the highest and the lowest latitudes the required overlapping could be reached with simple acquisitions with this minimal window dimension; the large FoV of STC, furthermore, allows in these regions to guarantee the planet coverage operating alternative orbits. In this manner the overlapping should be guaranteed not with the subsequent orbits but with the following ones. This strategy has three effects:

- The reduction of the DV avoiding overlapping for each orbit
- The use of greater CT swath reduces the number of images
- It improves the angular information needed for the mosaicking process and for the bundle adjustment procedures between subsequent acquisitions and between orbits.

As shown in **Figure 8** the cross track overlapping should be guaranteed, near polar regions, even without working 3 orbits every 4.

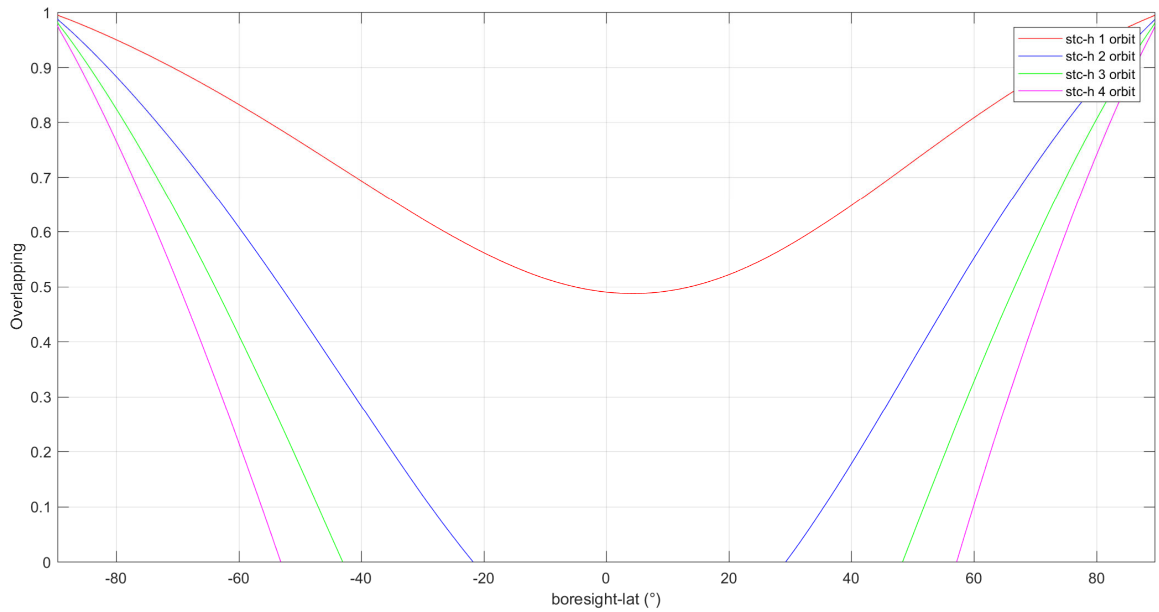


**Figure 8** – *Percentage of superposition (for the maximum cross track window size, 768 pixels), with respect to the boresight latitude, of the FoV of one orbit with the consecutive one (red line) and with the following three (blue and green and magenta lines), at the beginning of the mission (Aphelion 1).*

Considering that the assumption is based on the number of pixel (30) and not on the percentile of the CT dimension (which is variable) , the **Figure 9** underlines that using full CT FoV brings to an overlapping at periherm of more than 400 pixels at Aphelion 1 and it is possible to guarantee the full coverage of both pole regions by operating every other orbit .

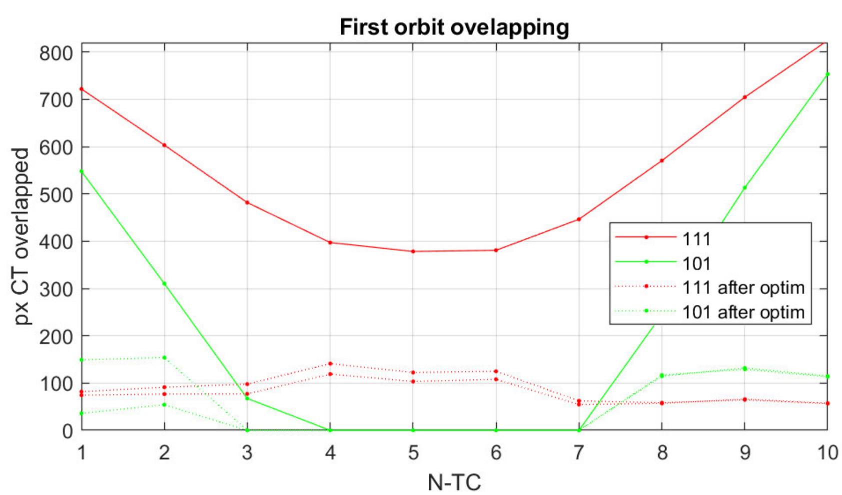


**Figure 9** *For each TC (corresponding to a section of orbit) the plot shows the evaluation of the CT overlapping considering the full FoV of STC (continuous lines) both in the case of operation for each orbit (red) or every other orbit (green). Dotted lines show the CT overlapping after optimization*.

After the optimization, the overlapping between consecutive or alternate orbits is limited to 128 px. The CT dimensions to be commanded for the first orbit of Aphelion 1 is the orbit shown in Figure 10 where it should be assumed to work every orbit in the first and last segments of the orbit corresponding to South and Nord poles.

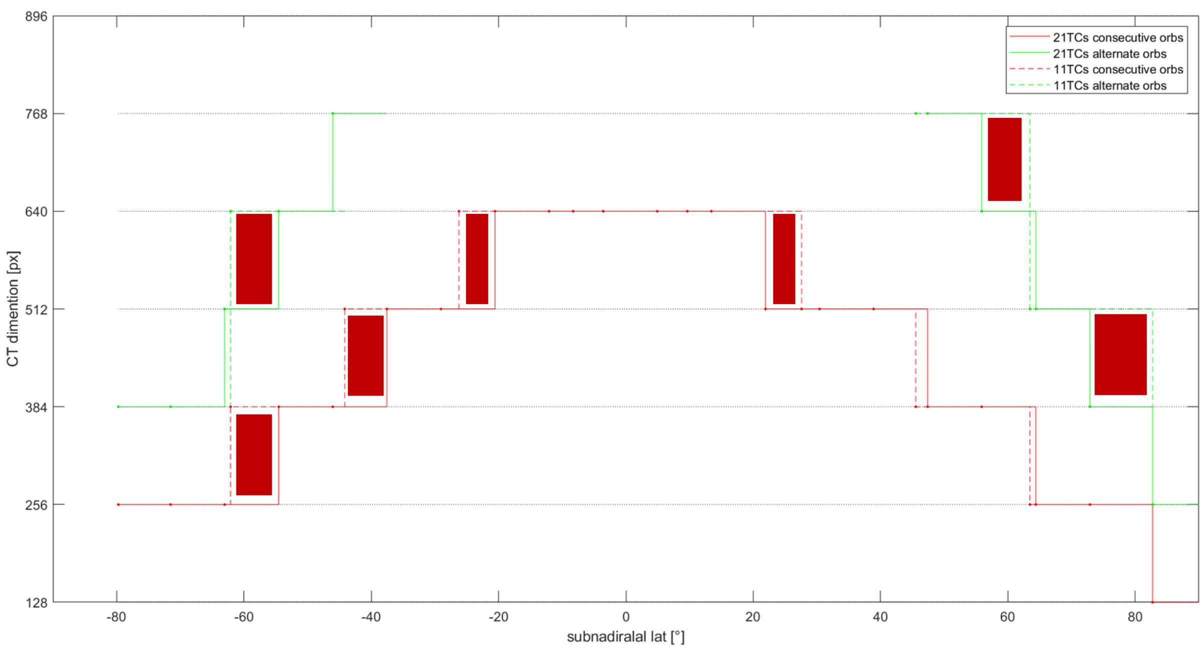


**Figure 10** *Optimized CT dimension of the PAN acquisition in the case of consecutive orbits (red) or alternate ones (green). Dotted line shows the optimization in case of an amount of 20 orbit section. Red regions represent the comparison between the 11 TCs planning and the 21 TCs planning. They underly the segments in which there is a strong increase in RT for the 11 TCs case which means they represent the gain in the choice of a greater number of TCs.*

**Figure 10** underlines in green the gain obtained assuming 21 TCs. As for the RT, even in this case, an increased number of orbit sections will provide an optimized strategy.
In **Figure 9** shows (dot lines) the number of pixels in overlapping for each section of orbit, it is possible to define the CT dimension to be commanded to reach these overlapping. In the case of 11 TCs it is shown in **Figure 11**.

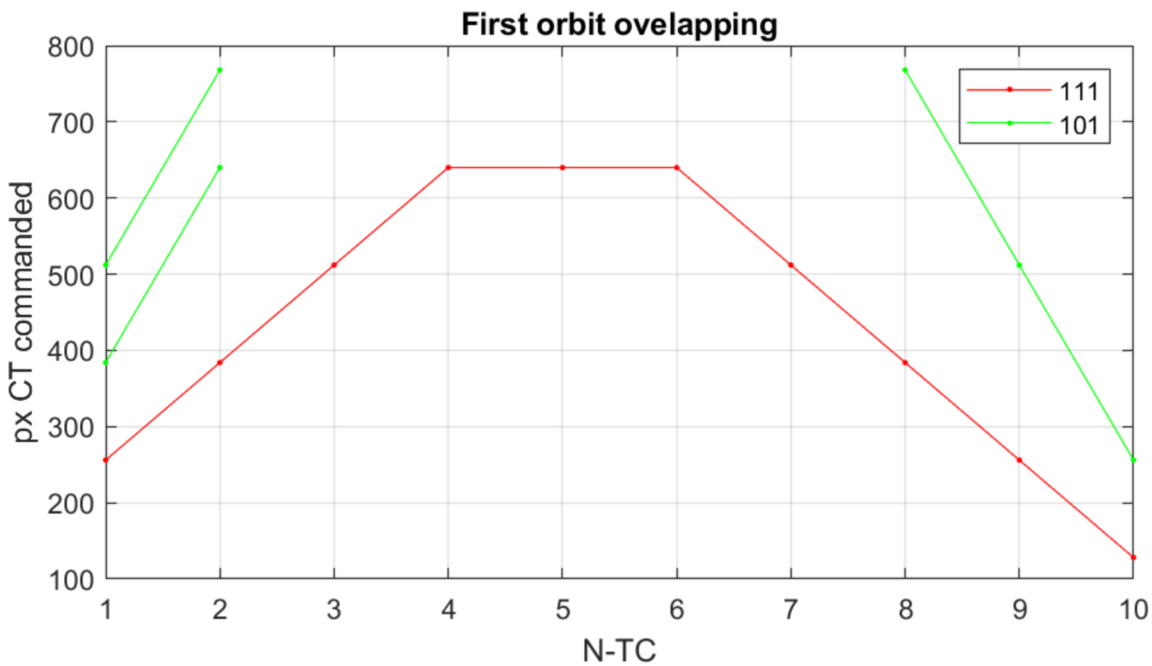


**Figure 11** *Evaluation of the CT dimension associated to each TC both in the case of operation for each orbit (red) or every other orbit (green).*

This process can be extended to all the orbits (which share the same segments definition). It is possible for each segment of the orbit to define the minimum CT dimension to guarantee the right overlapping with consecutive orbit and, for the first and last TCs, the overlapping for the odd orbits. The result of this analysis is shown in **Figure 12**(in the case of 11 TCs) and in **Figure 13** (in the case of 21 TCs).

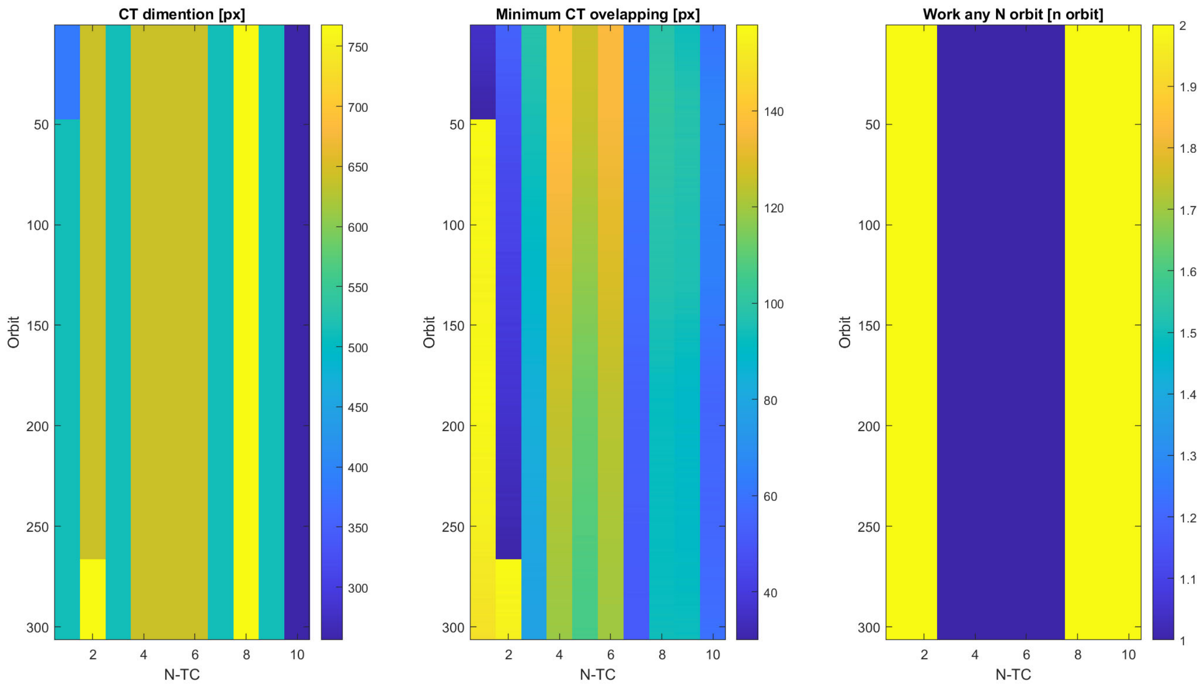


**Figure 12** *We evaluate for all the orbits (rows) of the first Aphelion (and for all the TCs) the following parameters: in (a) the CT dimension associated to each TC, in (b) the resulting overlapping with the subsequent orbit and in (c) if STC need to work at each orbit ( when the value is 1) or at alternative ones (when value is 2). Analysis considers using 11 TCs.*

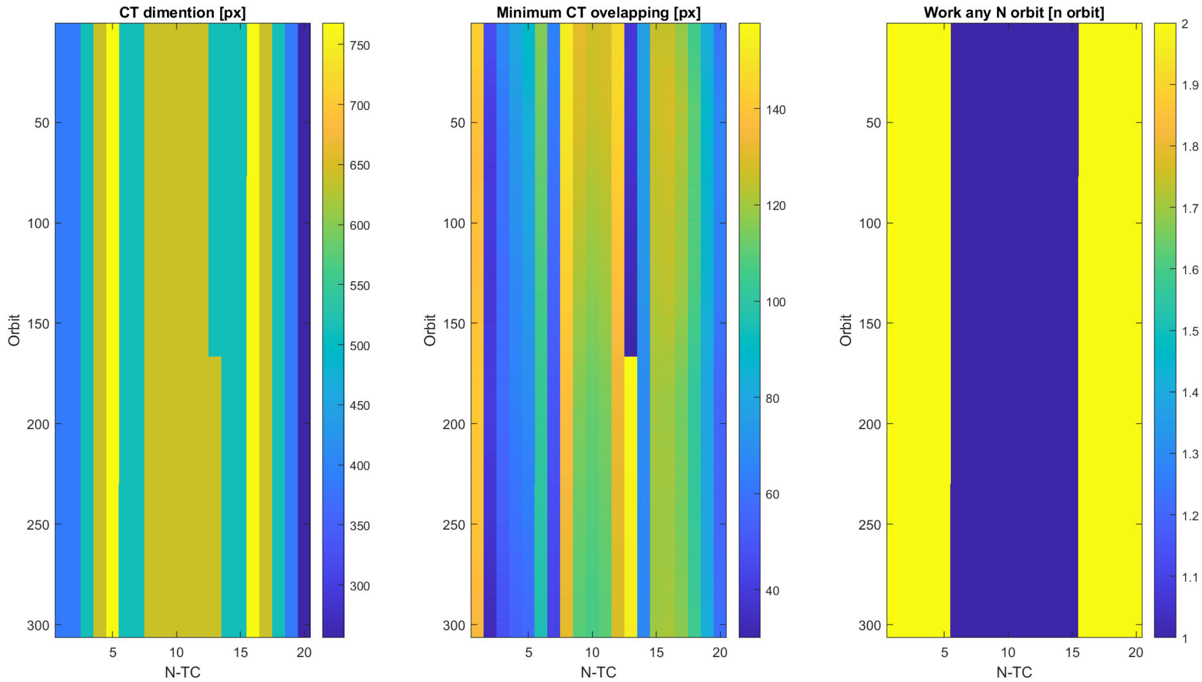


**Figure 13** *We evaluate for all the orbits of the first Aphelion (and for all the TCs) the following parameters: in (a) the CT dimension associated to each TC, in (b) the resulting overlapping with the subsequent orbit and in (c) if STC need to work at each orbit in the different orbit segments. Analysis considers a use of 21 TCs.*

# 5 DV production

The RT and CT dimensions defined and reported in previous sections, and the Compression Ratio assumed to be fixed to 7 (bit rate 2 bit/pix and IBR=32) are the parameter to be used for the DV estimate during the GM phase as defined in the Data Rate Evaluation reported in Section 6.

The data rate evaluation allows us to report the DV estimate for the main Aphelion's of the BepiColombo missions (see [RD. 8] for more details):

- Aphelion 0: 21 March – 20 April 2026;
- Aphelion 1: 16 June – 16 July 2026;
- Aphelion 2: 12 Sept – 12 Oct 2026;

We assume in this evaluation a full use of the GM even for all the Aphelion 0 (for a better comparison with the other cases).

Considering that all the parameters involved are dependent by the SC height (descending for all the mission) we report in **Table 4** the main parameters describing each aphelion and the minimum and mean duration of the orbit segments

| Ahepion | Min Long @periherm | Max Long @periherm | Max PoG AT @periherm | Min PoG AT @periherm | NTC | Duration Min | Duratio n Mean |
|---|---|---|---|---|---|---|---|
| # | [°] | [°] | [m] | [m] | | [s] | [s] |
| 0 | *3.1W* | *170.7E* | 61 | 58.9 | NTC=11 | 300 | 383 |
| | | | | | NTC=15 | 208 | 271.9 |
| | | | | | NTC=21 | 142 | 190.3 |
| | | | | | NTC=31 | 95 | 130 |
| 1 | *178 W* | *3.3W* | 55.3 | 53.6 | NTC=11 | 300 | 380.7 |
| | | | | | NTC=15 | 208 | 271.9 |
| | | | | | NTC=21 | 142 | 191.3 |
| | | | | | NTC=31 | 93 | 126.9 |
| 2 | *1.95W* | *176.4E* | 50.3 | 48.5 | NTC=11 | 292 | 374 |
| | | | | | NTC=15 | 202 | 266.9 |
| | | | | | NTC=21 | 138 | 186.85 |
| | | | | | NTC=31 | 90 | 124.5 |

**Table 4** *Table reports the main acquisition parameters of the GM observation strategy in case of continuous acquisitions for all the duration of the first three different Aphelion following the definition of the time windows reported in [RD. 8]. For each longitude and pixel on ground we reported the minimum and maximum values reached at periherm during the aphelion phase Last columns reports the minimum and mean duration of the orbit segments in the adoption of multiple.*

**Table 5** reports for each aphelion the DV estimate at the first and last orbit, the mean DV in the considered phase and the required value to maintain STC in GM for all the duration of the Aphelion.

| Ahepion | | DV 1 orbit | DV last orbit | Mean DV | Total DV | Gain |
|---|---|---|---|---|---|---|
| # | | [Mb/orb] | [Mb/orb] | [Mb/orbit] | Gb | % |
| 0 | NTC=11 | 189.81 | 202.83 | 197.65 | 60.48 | |
| | NTC=15 | 186.28 | 192.52 | 187.04 | 57.23 | 5.4 |
| | NTC=21 | 180.63 | 187.74 | 183.19 | 56.06 | 7.3 |
| | NTC=31 | 177.48 | 183.48 | 177.9 | 54.44 | 10.0 |
| 1 | NTC=11 | 238.18 | 250.39 | 242.46 | 74.19 | |
| | NTC=15 | 224.74 | 242.81 | 231.83 | 70.94 | 4.4 |
| | NTC=21 | 223.74 | 232.86 | 225.27 | 68.93 | 7 |
| | NTC=31 | 213.8 | 224.58 | 216.47 | 66.24 | 10.7 |
| 2 | NTC=11 | 265.44 | 290.05 | 275.99 | 84.45 | |
| | NTC=15 | 259.13 | 266.88 | 261.2 | 79.93 | 5.3 |
| | NTC=21 | 257.43 | 265.02 | 258.18 | 79 | 6.5 |
| | NTC=31 | 247.41 | 254.11 | 247.65 | 75.78 | 10.3 |

**Table 5** *Table reports the DV of the GM observation strategy in case of continuous acquisitions for all the duration of the first three different Aphelion following the definition of the time windows reported in [RD. 8]. Last column reports the percentile gain in the adoption of multiple TCs with respect to what was defined in [RD. 2].*

Old DV estimation (based on the old mission design and strategy and reported in [RD. 3]) reported a DV consumption for the GM of 130 Gb distributed in the Aphelion 1 and 2 where the instrument performance was in agreement with science objectives. The analysis demonstrated that the use of 15 TCs allows to reduce by 4% the DV consumption while this gain reaches the 7% for 21 TCs. This allows a DV (working at aphelion 1 and 2 ) of 147.9 Gb (with 21 TC) differently from the planned 158,6 Gb (with 11 TC). It is possible to unload part of the GM in the previous (0) Aphelion but the price is the spatial resolution.

**It is clear that instead of working during Aphelion 1 and 2 it should be possible to start the GM at second half of Aphelion 0, then, continue the acquisitions at Aphelion 1 and complete the GM at half of the Aphelion phase 2. This will allow to preserve part of the DV to the detriment of the 10% of the resolution for all the acquisition of Aphelion 0.**

# 6 Appendix: SIMBIOSYS Data Rate Evaluation

The document reports the Bit Rate evaluation for the SIMBIO-SYS channels as function of the formal parameters of the Science TCs. The first two sections give a detailed description of the parameters involved and the final equation calculation for the two Imaging Channels and for VIHI one.
The last section provides a summarizing table for the Data Rate computation.

## 6.1 STC & HRIC Channels

The acquisitions of the two imaging cameras of SIMBIOSYS, HRIC and STC, can be commanded through two modes. The associated TCs are reported in Table 6.

| Mode | HRIC | STC |
|---|---|---|
| Science | ZSS17102 (SIMB HRIC SCIENCE) | ZSS17202 (SIMB STC SCIENCE) |
| Science 1ms | ZSS171B2 (SIMB HRIC SCIENCE 1ms) | ZSS172B2 (SIMB STC SCIENCE 1ms) |

**Table 6** Science acquisition TCs for the two channels

The "Science" TCs are used for surface acquisitions (short integration times) and the "Science 1ms" TCs ones for the stellar ones; for this reason, the only difference in the structure of the modes is the integration time which, for HRIC is defined by PSS01501 in the first case and PSS015B1 in the latter; for STC it is defined by PSS0150 in the first case and PSS015B1 in the latter. This parameter has no impact in the evaluation of the data-rate.
The TCs allow to acquire a limited number $n$ of different windows (with $n = 4$ for HRIC and $n = 6$ for STC) of the FPGA with different Binning factors (in the case of HRIC) and Compression Ratio.
The cameras bitrate ($BR$) can be evaluated as:

$$BR = \frac{\sum_{h=1}^{n} Nbit_h}{RT} \quad (1$$

where $RT$ is the Repetition Time and $Nbit$ is the number of compressed bit generated by each single acquisition of the single window $h$.The two parameters can be defined as follows:

- The Repetition Time can be evaluated by the conversion of the PSS01601 (for HRIC) and PSS01501 (for STC) formal parameters. RAW values unit scale corresponds, in both the cases, to 5 ms which means that 200RAW commands the RT of 1s.
- The Number of bits produced by the single window $h$ is a function of the window parameters described in the next session.

### 6.1.1 Windows parameters

The next table reports the formal parameters for the science acquisition of HRIC and STC with their name and symbol used hereafter.
HRIC and STC science TCs share most of the PSSs a part the fact that HRIC cannot acquire more than 4 windows and STC has no possibility to acquire in binning mode.

| Paramter Name | Symbol | Windows | | | | | |
|---|---|---|---|---|---|---|---|
| | | w1 | w2 | w3 | w4 | w5 | w6 |
| Start Strip | $SS$ | PSS00501 | PSS00503 | PSS00505 | PSS00507 | PSS00509 | PSS00511 |
| End Strip | $ES$ | PSS00502 | PSS00504 | PSS00506 | PSS00508 | PSS00510 | PSS00512 |
| Start Row | $SR$ | PSS01101 | PSS01103 | PSS01105 | PSS01107 | PSS01109 | PSS01111 |
| End Row | $ER$ | PSS01102 | PSS01104 | PSS01106 | PSS01108 | PSS01110 | PSS01112 |
| Compression Ratio | $IBR$ | PSS00601 | PSS00602 | PSS00603 | PSS00604 | PSS00605 | PSS00606 |
| Binning | $b$ | PSS00201 | PSS00202 | PSS00203 | PSS00204 | | |

**Table 7** Parameters describing each HRIC and STC windows in terms of FPA position and compression. Blu parameters populate only HRIC TCs while red ones populate only STC TCs

For each window $i$, the number of bits for acquisition can be evaluated as

$$Nbit_i = A_i\, Bpp_i \quad (2$$

Where $A_i$ is the equivalent area corresponding to the number of pixel of the window considered after binning process (if required) and $B_{pp}$ are the bits per pixel commanded. The two values can be evaluated as follows:

- The equivalent area acquired can be calculate by the number of lines and rows as:

$$A_i = R_f\,(ER_i - SR_i + 1)(\,(ES_i - SS_i + 1) * 64) \quad (3$$

  Where $R_f$ (**always equal to 1 for STC**) is the resize factor due to the binning which, in the case of HRIC, can be calculated by following equation:

$$R_f = 2^{-2b_i}$$

- The Bit per pixel ($Bpp_i$) depends, instead, by window $IBR_i$ parameter following the summarization in next table:

| *Case* | $IBR$ (PSS value) | $Bpp$ |
|---|---|---|
| Bit-Packing | 0 | 14 |
| Lossless | 1 | 10 |
| Lossy | otherwise | $\frac{IBR_i}{16}$ |

**Table 8** *Conversion table between Inverse Bitrate commanded and the bit per pixel associated as reported in UMv10* [RD. 3*]*

## 6.2 VIHI Channels

The acquisitions of the VIHI spectrometer are commanded by the command ZSS17302 “SIMB VIHI Science”.
VIHI bitrate can be calculated by:

$$BR = F_B \frac{Nbit}{RT}$$

Where:

- The repetition time “$RT$" is defined by PSS01631 (same calibration curve of the RTs of the imaging cameras);

The Frame Binning ($F_B$) depends on PSS00208 following the conversion reported in

*Table 9*.

- $Nbit$ represents the number of bits produced by a single acquisition and can be calculated as:

$$Nbit = A\ Bpp$$

Where the equivalent area $A$ depends on: the window dimensions, the spectral and spatial binning while the bit per pixel ($Bpp$) depends, instead, only by the IBR defined in PSS00601 following same table reported as Table 8.
The equivalent area acquired can be calculated by the number of lines and rows as:

$$A = R_f^{spect}\ R_f^{spat}\ N_{rows}\ N_{cols}$$

Where $N_{rows}$ (representing the spectral direction) and $N_{cols}$ (representing the spatial direction) are rows and columns window dimensions defined respectively as (PSS01634-PSS01632+1) and (PSS01635-PSS01633+1); is important to note that if $R_f^{spect}$ is equal to 1 (spectral editing see table 4) $N_{rows}$ **must** be 128.
the Resize Factors due to the spectral and spatial binning are reported in the Binning conversion

| PSS | VIHI Spatial Binning (PSS00207) | Frame Binning (PSS00208) | Spectral binning (PSS00209) |
|---|---|---|---|
| Value | $R_f^{spat}$ | $F_B$ | $R_f^{spect}$ |
| 0 | 1 (no binning) | 1 (no binning) | 1 (no binning) |
| 1 | 0.5 (2x_Spatial_bin) | 0.5 | 1 Spectral_Editing |
| 2 | 0.125 (4x_Spatial_bin) | 0.125 | 0.5 (2x_Spectral_bin) |
| 3 | | | 0.125 (4x_Spectral_bin) |

**Table 9** *Conversion for all the Binning PSS of VIHI*

## 6.3 Summarization Table

The following tables summarize the procedure for the calculation of the Data-Rate, including the ID of the formal parameters, for the two imaging channels (Table 10) and for VIHI one (Table 11).

| | Paramter Name | Symbol | Windows | | | | | |
|---|---|---|---|---|---|---|---|---|
| | | | w1 | w2 | w3 | w4 | w5 | w6 |
| Formal Param. | Start Strip for win | $SS_i$ | PSS00501 | PSS00503 | PSS00505 | PSS00507 | PSS00509 | PSS00511 |
| | End Strip for win | $ES_i$ | PSS00502 | PSS00504 | PSS00506 | PSS00508 | PSS00510 | PSS00512 |
| | Start Row for win | $SR_i$ | PSS01101 | PSS01103 | PSS01105 | PSS01107 | PSS01109 | PSS01111 |
| | End Row for win | $ER_i$ | PSS01102 | PSS01104 | PSS01106 | PSS01108 | PSS01110 | PSS01112 |
| | Compression Ratio for win | $IBR_i$ | PSS00601 | PSS00602 | PSS00603 | PSS00604 | PSS00605 | PSS00606 |
| | Binning for win | $b_i$ | PSS00201 | PSS00202 | PSS00203 | PSS00204 | | |
| | Repetition Time | $RT$ | PSS01601 (for HRIC) and PSS01501 (for STC) | | | | | |
| Equations | Resize Factor | $R_f$ | $R_f = 2^{-2b_i}$ | | | | | |
| | Equivalent area | $A_i$ | $A_i = R_f\,(ER_i - SR_i + 1)(\,(ES_i - SS_i + 1) * 64)$ | | | | | |
| | Bit per pixel | $B_{pp_i}$ | $IBR_i$ | | | | $B_{pp_i}$ | |
| | | | 0 (Bit-Packing) | | | | 14 | |
| | | | 1 (Lossless) | | | | 10 | |
| | | | Otherwise (Lossy) | | | | $IBR_i$ / 16 | |
| | Bit per windows | $Nbit_i$ | $Nbit_i = A_i\,Bpp_i$ | | | | | |
| Bit Rate | | $BR$ | $BR = \frac{\sum_{h=1}^{n} Nbit_h}{RT}$ | | | | | |

**Table 10** Data Rate Evaluation for HRIC-STC Channel

| | Paramter Name | Symbol | Definition |
|---|---|---|---|
| Formal | Start Strip for win | $SC$ | PSS01632 |
| | End Strip for win | $EC$ | PSS01632 |
| | Start Row for win | $SR$ | PSS01633 |

| | | | | | | | |
|---|---|---|---|---|---|---|---|
| | End Row for win | $ER$ | PSS01635 | | | | |
| | Compression Ratio | $IBR$ | PSS00601 | | | | |
| | Repetition Time | $RT$ | PSS01631 | | | | |
| **Equations** | | | PSS VALUE | 0 | 1 | 2 | 3 |
| | Spatial Resize Factor | $R_f^{spat}$ | PSS00207 | 1 | 0.5 2x_Spat_bin | 0.125 4x_Spat_bin | |
| | Frame Binning | $F_B$ | PSS00208 | 1 | 0.5 | 0.125 | |
| | Spectral Resize Factor | $R_f^{spect}$ | PSS00209 | 1 | 1 Spectral_Editing | 0.5 2x_Spect_bin | 125 4x_Spect_bin |
| | Equivalent area | $A_i$ | $A = R_f^{spect}\, R_f^{spat}\, (ER - SR + 1)(EC - SC + 1)$ | | | | |
| | Bit per pixel | $B_{pp}$ | $IBR$ | | | $B_{pp}$ | |
| | | | 0 (Bit-Packing) | | | 14 | |
| | | | 1 (Lossless) | | | 10 | |
| | | | Otherwise (Lossy) | | | $IBR_i$ / 16 | |
| | Bit per windows | $Nbit$ | $Nbit = A\, Bpp$ | | | | |
| **Bit Rate** | | $BR$ | $BR = F_B \frac{Nbit}{RT}$ | | | | |

**Table 11** Data Rate Evaluation for VIHI Channel.